Review of Scientific Instruments

Biased quartz crystal microbalance method for studies of chemical vapor deposition surface chemistry induced by plasma electrons

Cite as: Rev. Sci. Instrum. **94**, 023902 (2023); https://doi.org/10.1063/5.0122143
Submitted: 22 August 2022 • Accepted: 19 January 2023 • Published Online: 09 February 2023
Published open access through an agreement with Linkopings universitet

Pentti Niiranen, Hama Nadhom, Michal Zanáška, et al.

AIP Publishing

Review of Scientific Instruments ARTICLE scitation.org/journal/rsi

Biased quartz crystal microbalance method for studies of chemical vapor deposition surface chemistry induced by plasma electrons

Cite as: Rev. Sci. Instrum. 94, 023902 (2023); doi: 10.1063/5.0122143
Submitted: 22 August 2022 • Accepted: 19 January 2023 •
Published Online: 9 February 2023

Pentti Niiranen,[1,a)] Hama Nadhom,[1] Michal Zanáška,[1] Robert Boyd,[1] Mauricio Sortica,[2] Daniel Primetzhofer,[2] Daniel Lundin,[1] and Henrik Pedersen[1]

AFFILIATIONS

[1] Department of Physics, Chemistry and Biology, Linköping University, SE-581 83 Linköping, Sweden
[2] Department of Physics and Astronomy, Uppsala University, Box 529, SE-751 20 Uppsala, Sweden

[a)] **Author to whom correspondence should be addressed:** pentti.niiranen@liu.se

ABSTRACT

A recently presented chemical vapor deposition (CVD) method involves using plasma electrons as reducing agents for deposition of metals. The plasma electrons are attracted to the substrate surface by a positive substrate bias. Here, we present how a standard quartz crystal microbalance (QCM) system can be modified to allow applying a DC bias to the QCM sensor to attract plasma electrons to it and thereby also enable *in situ* growth monitoring during the electron-assisted CVD method. We show initial results from mass gain evolution over time during deposition of iron films using the biased QCM and how the biased QCM can be used for process development and provide insight into the surface chemistry by time-resolving the CVD method. Post-deposition analyses of the QCM crystals by cross-section electron microscopy and high-resolution x-ray photoelectron spectroscopy show that the QCM crystals are coated by an iron-containing film and thus function as substrates in the CVD process. A comparison of the areal mass density given by the QCM crystal and the areal mass density from elastic recoil detection analysis and Rutherford backscattering spectrometry was done to verify the function of the QCM setup. Time-resolved CVD experiments show that this biased QCM method holds great promise as one of the tools for understanding the surface chemistry of the newly developed CVD method.

I. INTRODUCTION

Thin films of metals are important for several technological applications, such as catalysis and electrical contacts.[1] One of the most important methods for depositing metals is chemical vapor deposition (CVD), where a film is deposited on a surface by surface, and sometimes also gas phase, chemical reactions between precursor molecules.[2] A fundamental chemical reaction in most CVD processes for metals is a reduction reaction where the positive valence, i.e., ionic state, of the metal center in the precursor molecule is reduced to a zero-valent, metallic state. The reduction is done by a molecular reducing agent, providing electrons, by undergoing oxidation.[3] For very electropositive metals, the reduction is not favored thermodynamically, and powerful reducing agents and/or high temperatures are therefore needed to deposit a metallic film of, e.g., many of the first-row transition metals.[3]

We have recently presented an alternative CVD approach to thin metallic films where the free electrons in a plasma discharge are used for the reduction at the surface of the growing film.[4] This is done by applying a positive bias to the substrate holder to attract the plasma electrons to the substrate surface. We have demonstrated that the new CVD method uses plasma electrons for the deposition by showing that films are only deposited when a positive bias, attracting electrons, is used on the substrate holder, whereas no films are deposited when a negative bias, repelling electrons, is used. Moreover, the CVD method only functions on low-resistivity substrates, where the electron current from the plasma can be conducted away.[5] Although these results strongly suggest that the plasma

electrons are active in the surface chemistry, more advanced *in situ* measurements are needed to form a surface chemical model of the deposition chemistry in the new CVD method.

While several *in situ* methods are available for CVD,[6] few are as readily available for installation in almost any deposition chamber as the quartz crystal microbalance (QCM) sensor, which has a long history in the study of surface chemistry in CVD processes.[7] The QCM setup consists of a quartz crystal (a piezoelectric material) coated with metallic electrodes on the back and front sides of the quartz crystal. By applying an AC voltage to the metallic electrodes, a shear deformation of the quartz is induced, making it oscillate back and forth in an antiparallel fashion at its resonant frequency. The resonant frequency shifts when mass is adsorbed to or desorbed from the front electrode. Thus, the QCM can monitor instantaneous changes in adsorbed/desorbed mass by probing the shift in resonant frequency of the quartz crystal, according to Sauerbrey's equation,

$$\frac{\Delta m}{A} = -\frac{\sqrt{p_q G_q}}{2f_0^2}\frac{\Delta f}{n}, \tag{1}$$

where p_q is the density of quartz, G_q is the shear modulus of quartz, f_0 is the resonance frequency of the crystal, Δf is the frequency shift (in Hz), n is the nth overtone order (odd number integer), Δm is the change in mass, and A is the surface area of the quartz crystal.[8] In the present work, we refer to the $\Delta m/A$ term as "mass evolution" in arbitrary units due to the uncertainty in the exact surface area of the quartz crystal as a result of surface roughness. Since the deposited iron films are shown to be porous,[5] the film density will deviate from the bulk density of iron, meaning that reporting reliable QCM thickness values would need a calibration of the QCM with other techniques, e.g., spectroscopic ellipsometry, which has not been experimentally possible in our setup.

A challenge related to the newly developed CVD method is the requirement of a positive bias to attract plasma electrons to the substrate surface, which needs to be of low electrical resistivity to conduct away the electron current to the bias power supply. Most standard QCM crystals are coated with a thin layer of gold, which also makes them a low-resistivity surface, but additional biasing is not applied in conventional operation. Adding a positive bias to draw a current of plasma electrons would potentially also disturb the signal from the quartz oscillations, affecting the measurement. There are a few known modifications to the conventional QCM, where the objective has been to discriminate between neutral and charged species arriving at the crystal.[9–11] These reports focus on measuring the ionized flux fraction by either adding two grids in front of the crystal for electric bias or adding a strong magnetic field in front of the crystal in combination with directly biasing the quartz crystal electrode. The modified QCMs were operated in two different configurations: (i) no bias for measuring the total mass deposition rate R_t (proportional to the flux) and (ii) positive bias to repel all (positively charged) ions and measure the mass deposition rate of neutral particles R_n only. This allows the determination of the ionized flux fraction of the depositing particles.[12] It should, however, be noted that these modified QCMs were all constructed to repel plasma electrons from reaching the positively biased grid and/or crystal electrode. To our knowledge, no biased QCM has so far been employed to attract a flux of plasma electrons in a controlled manner.

Here, we present the modification of a conventional QCM system by the addition of a positive bias. We show that it can monitor film deposition during our electron-assisted CVD process and that the QCM crystal indeed functions as a regular substrate for the CVD process by characterizing the film deposited on the QCM crystal by electron microscopy, x-ray photoelectron spectroscopy (XPS), elastic recoil detection analysis (ERDA), and Rutherford backscattering spectrometry (RBS). We also show how the biased QCM system can be used to study the surface chemistry of the new CVD method by time-resolved deposition experiments, where the metal precursor and the plasma electrons are supplied sequentially.

II. APPARATUS

A commercial QCM sensor (Allectra) was used together with a gold coated quartz crystal (AT-cut, 6 MHz), connected to an external oscillator (MCVAC) and a readout unit TFM260 (BeamTec). The crystals were used as received and were not polished prior to

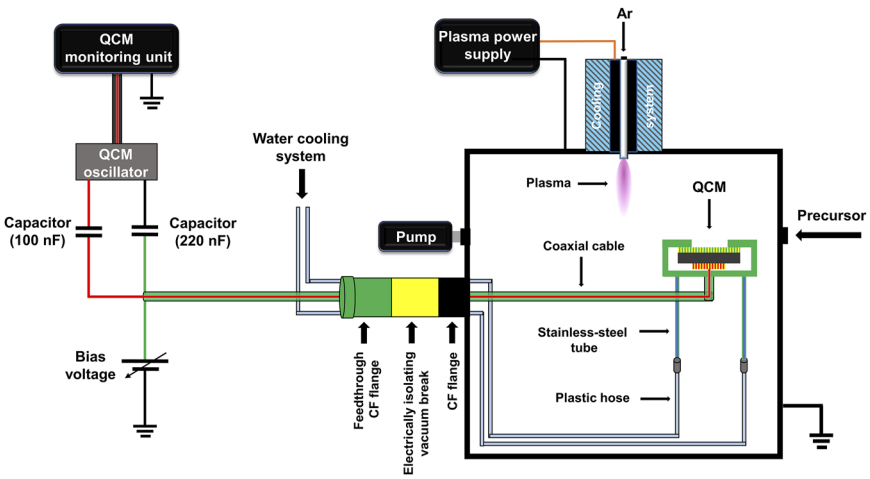

FIG. 1. Schematics of the experimental setup. The use of different colors in the electrical scheme of the QCM system is reflecting the different potentials (red—the QCM high-frequency signal, green—the bias voltage, black—ground).

deposition. A higher surface area was consequently expected and confirmed by atomic force microscopy (AFM), showing a root mean square roughness of 290 nm on a 50 × 50 μm^2 area. For that reason, we refer to the $\Delta m/A$ term, in Eq. (1), as "mass evolution" in arbitrary units due to the uncertainty in crystal surface area. In our QCM calculations, we still assume a perfectly flat surface. We are aware that surface roughness affects the absolute value of the areal mass density, although we want to stress that it does not affect the characteristics of the result, which ultimately allows us to establish qualitative trends.

The plasma CVD system used for the study has previously been described in detail[4] and is here modified with the biased QCM system. The experimental setup is schematically shown in Fig. 1. The electrical connection is based on the same principle as has been used in the case of the so-called gridless ion meter.[11,13] The ground connection of the QCM oscillator was connected to the top electrode of the crystal through a 220 nF capacitor, which allows for the QCM high-frequency single-ended signal to pass through and be measured while at the same time blocking the DC biasing voltage applied to the top electrode of the crystal from entering the QCM oscillator. Moreover, a 100 nF capacitor was connected in between bottom QCM electrode and the signal input of the QCM oscillator, in order to shield the QCM high-frequency signal from any external interference. In this configuration, the top crystal electrode could be readily biased without any influence on the QCM operation. The QCM sensor was connected to the QCM oscillator by a coaxial cable through a BNC electrical feedthrough ConFlat (CF) flange, which was electrically isolated from the grounded stainless-steel chamber by an isolating polytetrafluoroethylene (PTFE) vacuum break. The QCM sensor was also connected to a water-cooling/water-heating system, using electrically nonconductive PTFE hoses to electrically isolate the QCM sensor from the grounded stainless-steel chamber.

III. EXPERIMENTAL DETAILS

Iron films were deposited onto QCM crystals from ferrocene, bis(cyclopentadienyl)Fe(II) ($FeCp_2$), using plasma electrons as reducing agents. The deposition system setup and the experimental procedures are described in detail elsewhere.[4] Briefly, a custom-made stainless-steel vacuum chamber with a base pressure of 6 Pa was used with a titanium hollow cathode plasma source (with water-cooling system) mounted in the top lid of the vacuum chamber (Fig. 1). The QCM sensor was used instead of a substrate holder and was positioned downstream from the plasma source (Fig. 1) with a diagonal distance of 7 cm between the QCM electrode and the hollow cathode orifice. Such geometrical configuration allows the precursors to reach the QCM and adsorb at the surface prior to entering the main plasma bulk to minimize plasma chemical decomposition of the metal precursors as much as possible. To prevent unwanted condensation of precursor molecules on the QCM, the water-cooling system on the QCM was only used for a few selected experiments. Argon gas (140 sccm) and a DC power supply (5–20 W) were used to generate the plasma at a pressure of 33 Pa.

$FeCp_2$ powder was placed in a stainless-steel evaporation chamber, mounted on the deposition system, and purged with argon gas (35 sccm), while pumping on the deposition system for 1.5 h to remove the air from the bubbler. The $FeCp_2$ was then sublimed at 75 °C and the vapor was transported to the deposition chamber using argon (3 sccm) as carrier gas. A DC bias voltage in the range of −40 to +40 V was applied to the QCM sensor via a second DC voltage supply (Fig. 1). A multimeter was connected to the DC voltage supply to measure the electron current drawn from the plasma. The surrounding area of the QCM crystal plate and the outer walls of the QCM sensor was masked with Kapton tape to ensure that the measured electron current flows only through the top plasma-facing electrode of the QCM crystal.

Film deposition was carried out in two different manners: (1) either by continuously introducing $FeCp_2$ to the substrate while maintaining the plasma discharge or (2) by introducing the precursor and the plasma in sequential pulses, i.e., time-resolved deposition. Film depositions were carried out during 60 s (continuous CVD) and ~120 s (time-resolved CVD), in a total pressure range of 33–50 Pa, depending on the precursor flow. The QCM crystals were replaced after each deposition to always ensure similar surface conditions. The QCM data were collected and analyzed during depositions using the SQM160 software (Inficon) with a temporal resolution of one count/second.

Bulk morphology and composition of the deposited films were analyzed using scanning electron microscopy (SEM) and energy dispersive x-ray spectroscopy (EDS). Cross sections were prepared using a combined focused ion beam (FIB) and scanning electron microscope (SEM) (Crossbeam 1540 EsD, Zeiss) instrument. Prior to sectioning, a thin layer of Pt was deposited to protect the sample. Sections were first made with a Ga ion beam energy of 30 kV and a current of 1 nA with finer polishing using 200 and 50 pA. EDS mapping was performed with a GeminiSEM (Zeiss) fitted with an EDS detector (Oxford Instruments). The microscope was operated using an acceleration voltage of 10 kV and the sample was tilted to an angle of 45° to the electron beam for the electron beam to "see" the cross section and to better align with the EDS detector. A tilt compensation was applied to the image and map to account for this.

X-ray photoelectron spectroscopy (XPS) was used to analyze the elemental composition and chemical bonding in the deposited films using monochromatic Al K_α x rays. A charge neutralizer filament was used to compensate for the charge buildup effect. The conditions used for survey scans were as follows: energy range = 0–1200 eV, pass energy = 160 eV, step size = 0.1 eV, and x-ray spot size = 2 mm in diameter. A binding energy range of 20–40 eV (depending on the examined peak) was used for high-resolution spectra with a pass energy of 20 eV. Argon (0.5 keV) was used as the sputtering source. The C 1s peak with a value of 285 eV was used for calibration in all spectra. Gaussian–Lorentzian (GL) functions and a Shirley background were used to fit the experimental XPS data.

Time-of-Flight Heavy Ion Recoil Detection Analysis (ToF-HIERDA) was performed employing the 5 MV 15-SDH-2 Pelletron accelerator at Uppsala University,[14] where 36 MeV I^{8+} ions served as probing particles, incident under 67.5° with respect to the surface normal. Recoiling target nuclei were detected in a time-of-flight (ToF) telescope combined with a segmented gas ionization chamber[15] aligned 45° off the primary beam axis. ToF-energy coincidence spectra were transformed into depth profiles using the POTKU code.[16]

As a complement, and to compensate for the effects of multiple scattering caused by the Au-backing of the film of interest, which are deteriorating the depth profile,[17] we performed additional elastic backscattering spectrometry experiments. Specifically, we employed 6 MeV He^+ primary ions incident under 5° off the surface normal using the same accelerator system. Backscattered particles were detected under 170° scattering angle. Evaluation of backscattering spectra was done using the SIMNRA software package in combination with cross sections provided by the SigmaCalc package.[18,19] Data evaluation was subsequently performed in an iterative combinatorial approach providing depth-resolved information on all species present,[20] which can in turn be employed to obtain accurate areal mass densities for the probed film.

IV. RESULTS AND DISCUSSION

Film deposition experiments on the QCM crystals show that the film formation is highly dependent on the polarity of the applied bias voltage (Fig. 2), which is in agreement with our previous results, where 40 nm silver on Si(100) was used as a substrate.[4] In the present study, a positive bias voltage of +40 V, which attracts electrons from the plasma to the QCM crystal, led to a significant mass evolution, i.e., film deposition in a continuous CVD process, as seen in Fig. 2. In contrast, a negative bias voltage of −40 V, which repels plasma electrons at the QCM sensor, showed almost no increase in mass evolution. This suggests that plasma electrons are drawn to the surface of the QCM sensor, which then acts as the substrate in the current experimental setup.

To verify that the measured mass evolution with time is truly associated with film deposition, selected QCM crystals were analyzed post-deposition. Cross-section SEM analysis with compositional mapping by EDS for a QCM crystal that was used to study film deposition with continuous CVD at 10 W plasma power and +40 V bias is shown in Fig. 3. The EDS map shows that iron has been deposited on the quartz crystal. A platinum layer was deposited to prevent ion beam associated sample damage during preparation of the cross section. The cross-section micrograph shows that close to 1.8 μm film was deposited on the gold coated QCM crystal. The gold is not visible in the elemental mapping as a consequence of the resolution limits with EDS. The cross-section view reveals significant porosity and an ~160 nm thick void close to the substrate [Fig. 3(b)], indicating that continuous CVD with +40 V bias and 10 W plasma power is an unoptimized condition for film deposition.

In Fig. 2, it is shown that the modified QCM can be used to monitor mass evolution in time, using the quartz crystal as a substrate, ferrocene as the metal precursor and plasma electrons as reducing agents in continuous CVD. This opens for studying the surface chemistry more closely by monitoring growth during sequential precursor adsorption followed by plasma exposure. For this purpose, we employed a time-resolved CVD process where the Fe precursor and the plasma discharge were individually pulsed into the system with 5 s of $FeCp_2$ exposure followed by 5 s of plasma exposure. Note that no purge with inert gas, as done in atomic layer deposition (ALD), was used in between the $FeCp_2$ and the plasma pulses. The plasma discharge power was 10 W and the bias was set to +40 V. Figure 4 shows the mass evolution during film deposition with this time-resolved CVD process. We note that the mass gain is high during the early stage of the precursor pulse, indicating surface adsorption. It is followed by a slower mass gain after about 3 s, which may indicate an onset of saturation. During the entire plasma pulse, the QCM signal suggests a significant mass loss, albeit with a total mass gain after the full cycle.

To confirm that the overall mass evolution in Fig. 4, resulting in a net mass gain, is truly linked with deposition of Fe, a quartz

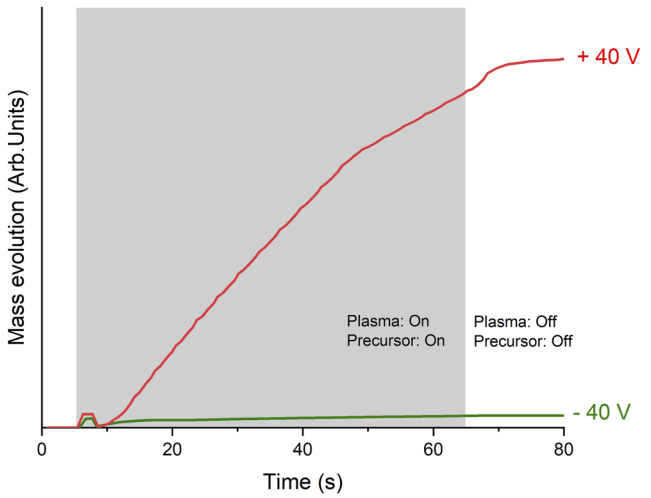

FIG. 2. Mass evolution at 10 W plasma power and +40 V (red) and −40 V (green) QCM bias voltage. The gray area corresponds to continuous deposition of iron, having both the plasma and the precursor on. The white areas correspond to no plasma and no precursor. A significant mass evolution can be seen at +40 V QCM bias voltage, while at −40 V no significant increase in mass evolution can be detected.

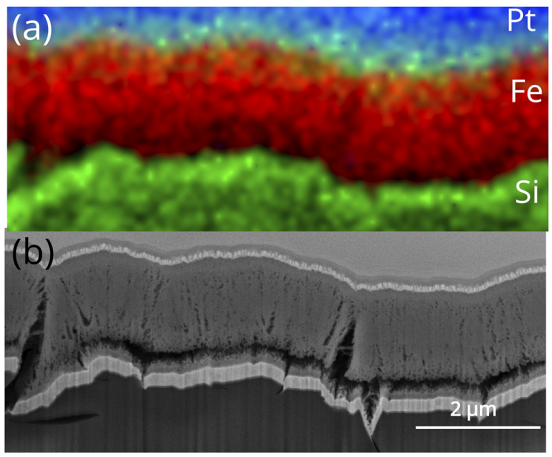

FIG. 3. (a) Elemental mapping by energy dispersive x-ray spectroscopy reveals that Fe has been deposited on the Au coated quartz crystal by continuous CVD at 10 W plasma power and +40 V QCM bias voltage and (b) cross-section scanning electron micrograph of the crystal reveals that the thickness of the Fe film is ~1.8 μm. Additionally, the cross-section scanning electron micrograph (b) of the crystal reveals that the film exhibits porous features and has an ~160 nm thick void close to the substrate.

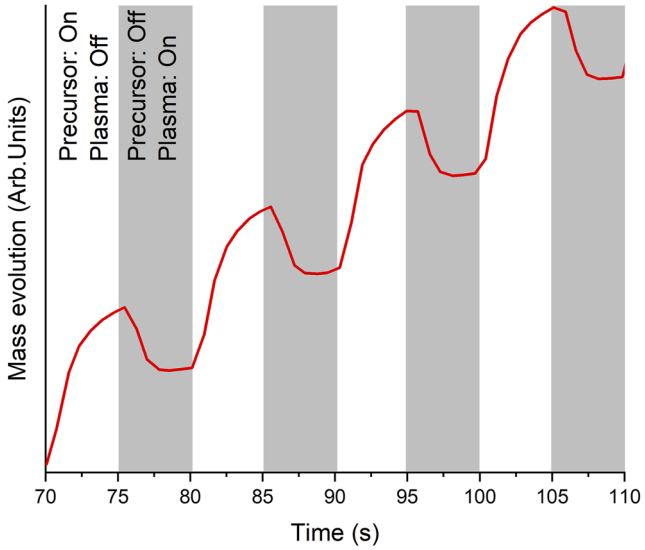

FIG. 4. Mass evolution during a time-resolved CVD process monitored by the modified biased QCM (+40 V) with a quartz crystal as a substrate, and where the precursor and plasma (10 W) are sequentially pulsed. White areas correspond to inflow of precursors and without any plasma discharge. The gray areas correspond to igniting and maintaining the plasma while not allowing the precursor into the deposition system.

crystal used for deposition at 10 W plasma power and +40 V QCM bias voltage was analyzed. An SEM-EDS map of the prepared cross section reveals the Fe film on the quartz substrate [Fig. 5(a)]. Compositional analysis of the film shows a high oxygen as well as iron content. Cross-section SEM analysis shows that close to an 850 nm film was deposited on the gold coated QCM crystal [Fig. 5(b)]. The cross-section micrograph also reveals some porosity, indicating that +40 V bias and 10 W plasma power is still not an optimized condition for film deposition.

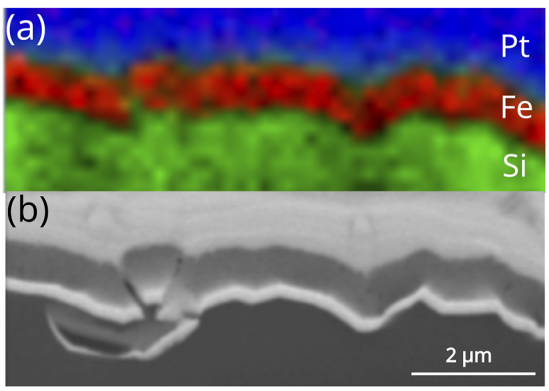

FIG. 5. Elemental mapping (a) by energy dispersive x-ray spectroscopy of time-resolved CVD deposited of Fe on the QCM crystal at 10 W plasma power and +40 V bias voltage and cross-section (b) scanning electron micrograph of the crystal reveal that the film exhibits porous features. The thickness of the film is ~850 nm.

High-resolution x-ray photoelectron spectroscopy (XPS) of a time-resolved film deposited on the gold coated QCM crystal with 10 W of plasma power and +40 V of bias, before and after sputter cleaning the surface, is given in Fig. 6. The Fe 2p shows peaks at 709.9–712 eV, corresponding to Fe–O.[21,22] Given that the samples were porous [Fig. 5(b)] and exposed to air for several days before being analyzed by XPS and due to the very oxyphilic nature of iron, oxidation is expected. In addition, film deposition was done in medium vacuum conditions, meaning that low levels of oxygen exposure are to be expected during deposition.[23] Therefore, the films were sputter-cleaned in the XPS chamber. After 1200 s of sputtering, shoulder peaks at 707.3 and 720.4 eV (Δ13.1 eV), likely corresponding to zero-valent Fe $2p_{3/2}$ and Fe $2p_{1/2}$, respectively, can be seen.[23,24] The compositional analysis by XPS of sputter-cleaned films deposited on the gold coated QCM crystal shows 38 at. % Fe, 26 at. % C, 32 at. % O, and 4 at. % N. The presence of the C impurities is most likely Cp ligands from the metal precursors remaining on the film surface being incorporated into the film.[25] Nitrogen is found as an impurity, likely due to the relatively high base pressure (6 Pa) or air trapped in the ferrocene evaporation chamber.

To investigate the reliability of the measured mass evolution, i.e., if the total shift of the resonant frequency is significantly altered by the introduction of an electron current, a quartz crystal with iron deposited at 10 W plasma power and +40 V QCM bias was analyzed by ERDA and RBS to estimate the areal mass density. The result was compared to the areal mass density given by the change in resonant frequency from the QCM. ERDA combined with RBS analysis showed an areal number density of 3.5×10^{18} atoms/cm^2. Assuming a flat surface of the quartz crystal in combination with the film composition values obtained from the ERDA/RBS (areal number density and relative elemental composition), the areal mass density equates to 1.25×10^{-4} g/cm^2, whereas the frequency shift in the QCM readout inserted into Eq. (1) suggested a value of 1.23×10^{-4} g/cm^2. This comparison suggests that the QCM data can be trusted even with the added bias signal. It should be noted that

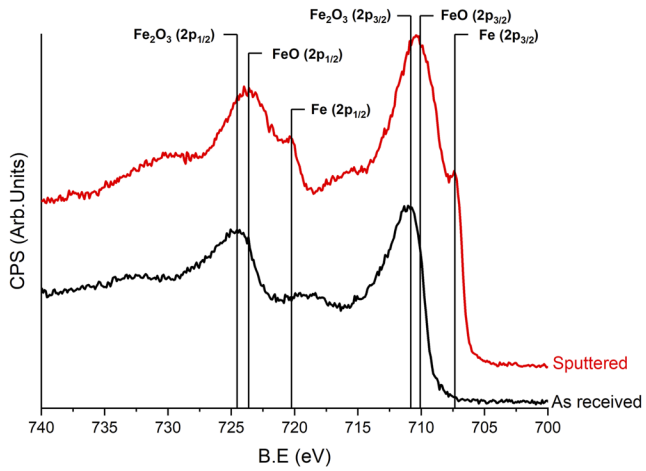

FIG. 6. High-resolution XPS spectra showing the iron spectral region of iron deposited on the QCM crystal at 10 W of plasma power and with a bias voltage of +40 V. Visible peaks are from metallic iron and iron oxide.

the QCM mass is based on a perfectly smooth surface, while we have measured a surface roughness of 290 nm on an area of 50 × 50 μm^2 by AFM.

We have so far established that the overall net mass gain in the continuous process (Fig. 2) and the time-resolved process (Fig. 4) indeed seems to generate reasonable values. However, a more detailed analysis of the observed trends during the different stages of precursor on/plasma off as well as precursor off/plasma on requires an analysis of the measured signal from the modified QCM. It is paramount to explore any potential interference due to the electron current drawn from the plasma to the crystal, which could result in a perturbed measurement of the crystal resonant frequency. We therefore exposed the QCM to a continuous (Fig. 7) and pulsed (Fig. 8) flow of plasma electrons, without any flow of $FeCp_2$ in the chamber. The plasma power was varied between 5 and 20 W to achieve an increase of the electron flux to the surface of the QCM while the QCM bias voltage was maintained at +40 V. For all explored plasma powers, the measured frequency shift increases with increased plasma power. This is in line with the increased electron current through the surface. In a QCM, the change in areal mass density scales inversely with the oscillation frequency ($\Delta m/A \propto -\Delta f$), implying that an event that appears to be a mass loss is expected when the plasma is ignited.

From the overall relative frequency shifts between 0 and 180 s in Fig. 7 and between 0 and ~140 s in Fig. 8, it is seen that there is in fact no net mass gain. This is expected since the precursor flow was off for the entire time. The recorded relative frequency shifts during "plasma on" are likely related to the plasma electron current momentarily disturbing the QCM measurements, although no permanent error in the measurement persists after this phase. This implies that the trend in mass change per unit time is hard to resolve while allowing an electron current to pass through at the initial plasma exposure between 5 and 20 W during the measurement, as seen in Figs. 7 and 8. However, we note from this that other regimes when the plasma is off and when the oscillation frequency has stabilized are reliable.

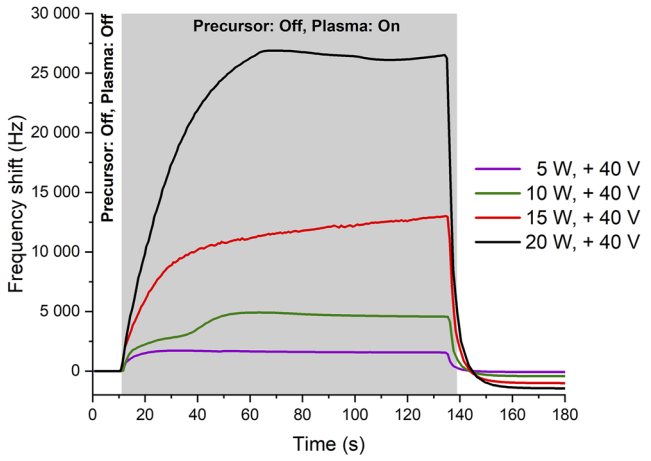

FIG. 7. Probing of the oscillation frequency by continuously exposing the QCM to plasma electrons at a QCM bias voltage of +40 V and plasma power of 5–20 W during 125 s. When the plasma is ignited (gray area), a positive shift of the oscillation frequency can be seen, which stabilizes at a constant frequency. When the plasma is turned off (white areas) at 135 s, the oscillation frequency of the QCM is restored.

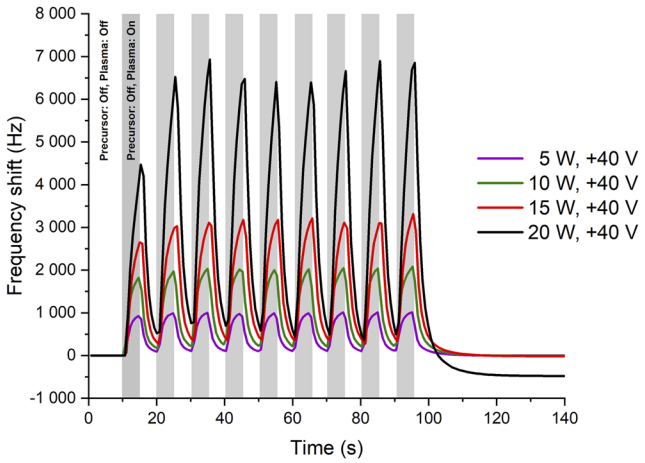

FIG. 8. Measurement of signal perturbations from time-resolved plasma pulses of 5 s (gray areas), followed by 5 s of neither allowing precursors into the chamber nor igniting the plasma (white areas). A plasma power between 5 and 20 W in combination with a fixed QCM bias voltage of +40 V was used in a period of 120 s.

To better understand the time-resolved CVD process (Fig. 4), it is also here necessary to understand how the oscillation frequency of the QCM behaves when pulsing plasma electrons on the QCM crystal in contrast to exposing it to a continuous flow of plasma electrons. While varying the plasma power (5–20 W) with a constant bias voltage of +40 V, we explored this by pulsing the plasma in 5 s pulses on the QCM crystal with no flow of $FeCp_2$ in the chamber. This was followed by 5 s with neither plasma nor $FeCp_2$. In line with the signal behavior during a continuous plasma (Fig. 7), the plasma exposure perturbs the QCM signal, contributing to a positive frequency shift that subsides when the plasma is turned off. The magnitude of the frequency shift increases with increasing plasma power (Fig. 8), which is in line with exposure to a continuous plasma (Fig. 7). We conclude from Figs. 7 and 8 that the change in oscillation frequency is not to be trusted during the plasma pulse until it has stabilized. When stabilized, no signal perturbations are present. Although, looking at the overall frequency signal, a negative shift of the frequency signal can be seen in Fig. 7, where the shift increases with plasma power, in Fig. 8, an overall negative frequency shift can be seen only for 20 W plasma power. The suggested mass gain (negative frequency shift) can be attributed to slight sputtering from the Ti hollow cathode plasma as observed earlier in the same deposition system.[4,5] Alternatively, it could be due to precursor molecules adsorbed on the chamber walls, desorbing during the Plasma: On-step and re-adsorbing on the QCM.

Additional experiments were carried out, employing a negative bias voltage to the QCM (repelling the electrons), during continuous plasma exposure, to further probe the origin of the observed QCM signal disturbance. It resulted in an exceedingly low frequency shift (Δ15 Hz) in comparison to those seen when employing a positive bias voltage with a continuous plasma exposure (up to Δ27 500 Hz).

The flux of negative charge carriers is clearly behind the significant frequency shift during plasma exposure by generating electrical noise. Alternatively, it may lead to resistive heating of the QCM crystal upon drawing an electron current through it. We explored this by cooling the QCM crystal to 5 °C using the water-cooling system of the QCM setup (Fig. 1) and exposing it to a continuous flow of plasma electrons. This resulted in a reduced, but not eliminated, frequency shift (Fig. 9). Consequently, we assume that, at least partially, the signal perturbation is due to momentary heating by the plasma electrons. It has earlier been shown that even small temperature gradients may generate apparent mass changes in QCM measurements.[26] Please note that not only electrons but also negative ions may be accelerated toward the surface of the QCM upon applying a positive bias. We believe that the negative ion density is very small in comparison to the electron density, although this remains to be verified in a future study.

It thus seems that a stabilizing step is needed in between the plasma pulse and the precursor pulse to be able to study the phenomenon of surface adsorption during the precursor step. We note that by cooling the QCM, the perturbation of the signal is reduced but not fully eliminated and that excessive cooling of the QCM may lead to unwanted precursor condensation rather than adsorption on the QCM surface. We therefore employed a stabilizing step without cooling the QCM in a time-resolved deposition of iron. The QCM data in Fig. 10 indicate a saturation of the surface adsorption, ~2 s into the precursor purge (white areas). Ensuing the saturation event, the plasma pulse (gray areas) shows a decrease in mass evolution, which is shown to be connected to a signal perturbation by the plasma in Fig. 8. In the following step, precursor off/plasma off (blue areas), the signal starts to stabilize, which is in line with the perturbation connected to the plasma electrons. This kind of measurement, where the precursor and the plasma are sequentially introduced, allows the possibility to study the surface adsorption of the electron-assisted CVD process where plasma electrons are used as reducing agents more closely. To study the reduction step, a combination of multiple *in situ* techniques will be necessary to understand what happens when the plasma electrons interact with the surface. However, this is outside the scope of the present study.

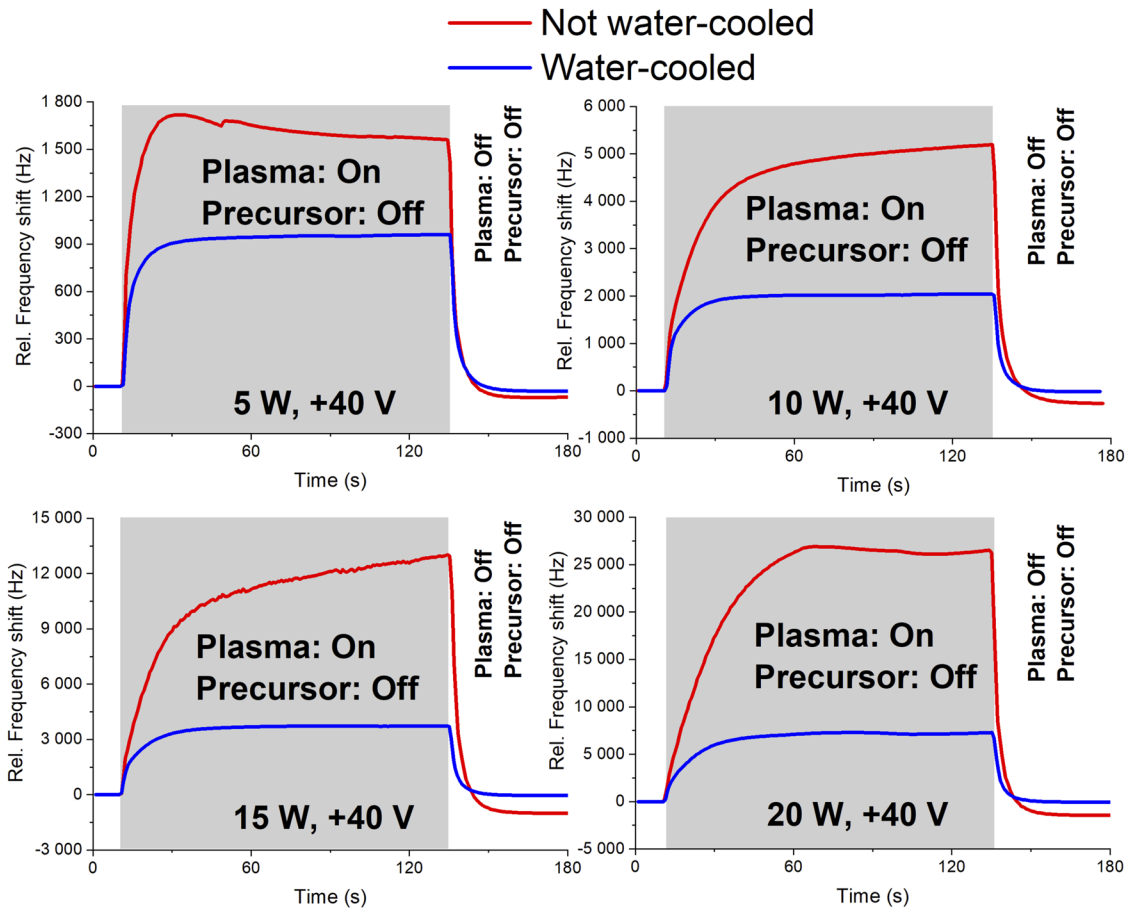

FIG. 9. Measurement of signal perturbations from a continuous plasma exposure. During all measurements, a plasma power between 5 and 20 W in combination with a fixed QCM bias voltage of +40 V was used. The white areas correspond to when no plasma is ignited, nor no precursors are allowed to flow into the deposition chamber. The gray areas correspond to when the plasma is ignited but no precursors are allowed to flow into the chamber.

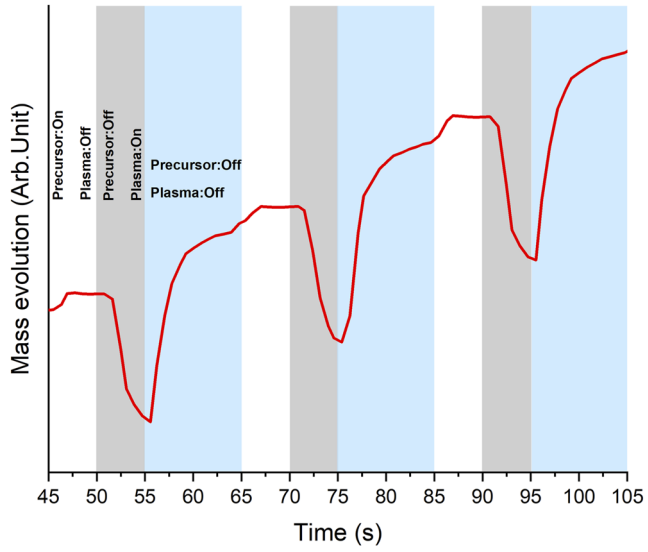

FIG. 10. Time-resolved deposition at 10 W and +40 V QCM bias voltage. The white areas show the precursor exposure (plasma off), indicating surface adsorption that goes to surface saturation after ~2 s. The gray areas show the plasma pulse, showing a significant mass loss, which are assumed to be due to a perturbation of the QCM signal due to plasma exposure (see Fig. 8). The blue areas show a regime where no precursor is allowed into the system and no ignition of the plasma and are referred to as the stabilizing step for the QCM signal prior to the surface adsorption step.

From monitoring the growth in continuous and time-resolved CVD, it is found that the QCM indeed can be used to monitor net mass evolution in time. During the time the plasma is ignited, the measurement is, however, perturbed, which we showed for both continuous and time-resolved processes. We ascribe this perturbation to drawing an electron current through the QCM crystal, causing resistive heating. To circumvent the perturbation of the high-frequency signal during the time-resolved process, a stabilizing step is needed after each plasma pulse. This means that characteristics, such as surface saturation, can be probed. For the net mass gain (i.e., growth rate), no stabilizing steps are needed since the resonant frequency drops back down and since no disturbance persists. In addition to net mass gain and surface saturation, the QCM can be useful as a tool to unveil the surface reactions when combined with, e.g., mass spectrometry. Through this approach, we can study both the adsorption of the precursor and the reaction by-products. The use of the biased QCM system together with a time-resolved CVD approach shows the potential of the QCM system to unveil details of the surface chemistry of this new CVD method in combination with other *in situ* techniques.

V. CONCLUSIONS

By modifying the electrical connections in a standard QCM sensor, we show that it is possible to add a positive bias to the QCM sensor to attract plasma electrons to the QCM crystal and thereby use this modified device for *in situ* growth monitoring during a recently developed electron-assisted CVD process. By analysis of the QCM crystals post-deposition, we show that iron films, contaminated by oxygen and carbon, are deposited. The ability of the biased QCM system to unveil details about the surface chemistry as well as to monitor film deposition is demonstrated by continuous and time-resolved CVD experiments. However, the results suggest that a stabilization time step for the high-frequency single-ended QCM signal is needed after being exposed to an electron current. This modified QCM method thus shows great potential for investigating the surface chemistry of this newly developed CVD method.

ACKNOWLEDGMENTS

Financial support from the Swedish Research Council (VR) under Contract Nos. 2015-03803 and 2019-05055, from the Swedish Foundation for Strategic Research under Contract No. SSF-RMA 15-0018, and from the Lam Research Corporation is gratefully acknowledged. The authors thank Petter Larsson at Ionautics AB, Sweden, for technical support during the measurements.

AUTHOR DECLARATIONS

Conflict of Interest

The authors have no conflicts to disclose.

Author Contributions

Pentti Niiranen: Data curation (lead); Investigation (lead); Project administration (equal); Resources (equal); Validation (lead); Visualization (equal); Writing – original draft (equal); Writing – review & editing (lead). **Hama Nadhom**: Methodology (equal); Resources (equal); Visualization (equal); Writing – original draft (lead); Writing – review & editing (equal). **Michal Zanaska**: Methodology (equal); Resources (equal); Software (supporting); Writing – review & editing (equal). **Robert Boyd**: Data curation (equal); Investigation (equal); Writing – original draft (equal); Writing – review & editing (equal). **Mauricio Sortica**: Data curation (equal); Investigation (equal); Resources (equal); Writing – original draft (equal). **Daniel Primetzhofer**: Data curation (equal); Investigation (equal); Resources (equal); Writing – original draft (equal). **Daniel Lundin**: Conceptualization (equal); Funding acquisition (equal); Project administration (equal); Supervision (equal); Writing – original draft (equal); Writing – review & editing (equal). **Henrik Pedersen**: Conceptualization (equal); Funding acquisition (equal); Project administration (equal); Supervision (lead); Writing – original draft (equal); Writing – review & editing (equal).

DATA AVAILABILITY

The data that support the findings of this study are available from the corresponding author upon reasonable request.

REFERENCES

[1] S. Krishna, *Handbook of Thin Film Deposition Processes and Techniques, Principles, Methods, Equipment and Applications*, 2nd ed. (Noyes Publications, William Andrew Publishing, Norwich, NY, 2002).

[2]K. L. Choy, Prog. Mater. Sci. **48**, 57 (2003).
[3]T. J. Knisley, L. C. Kalutarage, and C. H. Winter, Coord. Chem. Rev. **257**, 3222 (2013).
[4]H. Nadhom, D. Lundin, P. Rouf, and H. Pedersen, J. Vac. Sci. Technol. A **38**, 033402 (2020).
[5]H. Nadhom, R. Boyd, P. Rouf, D. Lundin, and H. Pedersen, J. Phys. Chem. Lett. **12**, 4130 (2021).
[6]K. Knapas and M. Ritala, Crit. Rev. Solid State Mater. Sci. **38**, 167 (2013).
[7]J. W. Elam, M. D. Groner, and S. M. George, Rev. Sci. Instrum. **73**, 2981 (2002).
[8]D. Johannsmann, *The Quartz Crystal Microbalance in Soft Matter Research: Fundamentals and Modeling* (Springer International Publishing, Heidelberg, NY, Dordrecht, London, 2015).
[9]K. M. Green, D. B. Hayden, D. R. Juliano, and D. N. Ruzic, Rev. Sci. Instrum. **68**, 4555 (1997).
[10]S. M. Rossnagel and J. Hopwood, Appl. Phys. Lett. **63**, 3285 (1993).
[11]T. Kubart, M. Čada, D. Lundin, and Z. Hubička, Surf. Coat. Technol. **238**, 152 (2014).
[12]D. Lundin, M. Čada, and Z. Hubička, Plasma Sources Sci. Technol. **24**, 035018 (2015).
[13]T. Shimizu, M. Zanáška, R. P. Villoan, N. Brenning, U. Helmersson, and D. Lundin, Plasma Sources Sci. Technol. **30**, 045006 (2021).
[14]P. Ström and D. Primetzhofer, J. Instrum. **17**, P04011 (2022).
[15]P. Ström, P. Petersson, M. Rubel, and G. Possnert, Rev. Sci. Instrum. **87**, 103303 (2016).
[16]K. Arstila, J. Julin, M. I. Laitinen, J. Aalto, T. Konu, S. Kärkkäinen, S. Rahkonen, M. Raunio, J. Itkonen, J.-P. Santanen, T. Tuovinen, and T. Sajavaara, Nucl. Instrum. Methods Phys. Res., Sect. B **331**, 34 (2014).
[17]E. Pitthan, M. V. Moro, S. A. Corrêa, and D. Primetzhofer, Surf. Coat. Technol. **417**, 127188 (2021).
[18]M. Mayer, AIP Conf. Proc. **475**, 541 (1999).
[19]A. F. Gurbich, Nucl. Instrum. Methods Phys. Res., Sect. B **371**, 27 (2016).
[20]M. V. Moro, R. Holeňák, L. Zendejas Medina, U. Jansson, and D. Primetzhofer, Thin Solid Films **686**, 137416 (2019).
[21]A. G. Sault, Appl. Surf. Sci. **74**, 249 (1994).
[22]D. L. Peng, K. Sumiyama, M. Oku, T. J. Konno, K. Wagatsuma, and K. Suzuki, J. Mater. Sci. **34**, 4623 (1999).
[23]G. B. Rayner, N. O'Toole, J. Shallenberger, and B. Johs, J. Vac. Sci. Technol. A **38**, 062408 (2020).
[24]J. F. Moulder, W. F. Stickle, P. E. Sobol, and K. D. Bomben, *Handbook of X-ray Photoelectron Spectroscopy*, 2nd ed. (Perkin-Elmer Corporation, Eden Prairie, MN, 1992).
[25]A. Gasparotto, G. Carraro, C. Maccato, and D. Barreca, Phys. Status Solidi A **214**, 1600779 (2017).
[26]M. N. Rocklein and S. M. George, Anal. Chem. **75**, 4975 (2003).